Supplemental material for: Superanomalous skin-effect and enhanced absorption of light scattered on conductive media

A. Vagov[1], I. A. Larkin[2], M. D. Croitoru[3], and V. M. Axt[1]
[1] *Theoretische Physik III, Universität Bayreuth, 95440 Bayreuth, Germany*
[2] *Institute of Microelectronics Technology Russian Academy of Sciences, 142432 Chernogolovka, Russia and*
[3] *Universidade Federal de Pernambuco, 50670-901 Recife, Pernambuco, Brazil*

I. ELECTROMAGNETIC FIELD INSIDE THE METAL

A. Non-local bulk response

The material response of a bulk metal is most conveniently formulated in Fourier space as a relation between the polarization and the electric field:

$$\boldsymbol{P}_{\omega,\boldsymbol{k}} = \widehat{\chi}_{\omega,\boldsymbol{k}}\, \boldsymbol{E}_{\omega,\boldsymbol{k}}, \tag{1}$$

where the bulk susceptibility tensor $\widehat{\chi}$ can be further decomposed into longitudinal and transverse parts according to:

$$\chi^{\alpha\beta}_{\omega,\boldsymbol{k}} = \chi^{\mathrm{tr}}_{\omega,k}\left(\delta_{\alpha\beta} - \frac{k_\alpha k_\beta}{k^2}\right) + \chi^{\ell}_{\omega,k}\frac{k_\alpha k_\beta}{k^2} = \chi^{\mathrm{tr}}_{\omega,k}\delta_{\alpha\beta} + \bar{\chi}_{\omega,k}\frac{k_\alpha k_\beta}{k^2}, \tag{2}$$

with $\bar{\chi} = \chi^{\ell} - \chi^{\mathrm{tr}}$ and $k = |\boldsymbol{k}|$. The term involving $\bar{\chi}$ yields in real space and time a contribution to the susceptibility tensor:

$$\begin{aligned}\int \frac{\mathrm{d}^3k}{(2\pi)^3}\int \frac{\mathrm{d}\omega}{2\pi}\, k_\alpha k_\beta\, \frac{\bar{\chi}_{\omega,k}}{k^2}\, e^{i(\boldsymbol{k}\cdot\boldsymbol{r}-\omega t)} &= \frac{1}{i}\frac{\partial}{\partial r_\alpha}\frac{1}{i}\frac{\partial}{\partial r_\beta}\underbrace{\int \frac{\mathrm{d}^3k}{(2\pi)^3}\int \frac{\mathrm{d}\omega}{2\pi}\,\frac{\bar{\chi}_{\omega,k}}{k^2}\, e^{i(\boldsymbol{k}\cdot\boldsymbol{r}-\omega t)}}_{=:f(t,r)} \\ &= -\frac{\partial}{\partial r_\alpha}\frac{r_\beta}{r}\frac{\partial}{\partial r} f(t,r) = -\frac{\delta_{\alpha\beta}}{r}f' - \frac{r_\alpha r_\beta}{r}\frac{\partial}{\partial r}\big(\frac{1}{r}\,f'\big),\end{aligned} \tag{3}$$

where we have used that the Fourier-transform of a function that only depends on $k = |\boldsymbol{k}|$ is in real space a function of $r = |\boldsymbol{r}|$. Thus the susceptibility tensor in real space and time reads:

$$\chi(t,\boldsymbol{r})_{\alpha\beta} = \delta_{\alpha\beta}\Big(\chi^{\mathrm{tr}}(t,r) - \frac{f'(t,r)}{r}\Big) - \frac{r_\alpha r_\beta}{r}\frac{\partial}{\partial r}\frac{f'(t,r)}{r} \tag{4}$$

Transforming (1) to real space and time we obtain:

$$\boldsymbol{P}(t,\boldsymbol{r}) = \int \mathrm{d}^3r' \int \mathrm{d}t'\, \chi(t-t',\boldsymbol{r}-\boldsymbol{r}')\, \boldsymbol{E}(t',\boldsymbol{r}'), \tag{5}$$

which is clearly a non-local relation in space and time. Indeed, (5) can be interpreted such that a field $\boldsymbol{E}$ at a space-time point $\boldsymbol{r}'$, t' is the source of a polarization that spreads away from the source point until it reaches the point $\boldsymbol{r}$, t. The integration in (5) means that the polarization at $\boldsymbol{r}$, t is the superposition of all contributions that spreading away from their respective source points have reached $\boldsymbol{r}$ at time t.

B. Specular reflection model of the surface

When a metallic half-space $z < 0$ is bounded by a surface to a dielectric occupying the region $z > 0$ it is clear that there cannot be any sources for a metallic response outside the metal since the electromagnetic response in the dielectric is local in space and time. Thus an obvious modification of (5) is that the z' integration can extend only over the half-space $z' < 0$. However, further modifications are necessary to account for the presence of a surface. In the specular reflection model it is assumed that each point $\boldsymbol{r}'$, t' inside the metal is, as in the bulk, a source of a polarization that at time t' starts spreading away from this point. When this polarization wave reaches the surface

it cannot propagate into the region outside the metal and thus gets reflected. Therefore, at each point $\boldsymbol{r}$, t one needs to collect not only the contributions to $\boldsymbol{P}$ that have reached this point directly propagating away from $\boldsymbol{r}'$, t' but also the parts that have been reflected at the surface. Noting that $\dot{\boldsymbol{P}}$ represents a current we have to enforce the boundary condition that its normal component is zero at the surface since otherwise there would be a current flowing into the region $z > 0$ which is prevented by the high potential barrier for the electrons in the metal. The condition $\dot{P}_\perp = 0$ at the interface can be regarded as an additional boundary condition (ABC) of the type proposed by Pekar.[1] Here, it appears as a consequence of the specular reflection model (SRM) for metal electrons. This condition can be easily ensured by superimposing the corresponding component of the reflected wave with a minus sign. For the tangential component the situation is different since in the $x-y$-plane the polarization can freely oscillate. Thus the reflection should take place like the reflection of a string with an open end, i.e., the corresponding component of the reflected wave should be superimposed with a plus sign. In the specular reflection model restricting the source points to the half-space $z' < 0$ and superimposing the reflected polarization waves to the waves that would propagate away from these source points in a bulk system, constitutes the description of the material response of a metallic half-space. Altogether these ideas can be summarized by the following material equation:

$$\boldsymbol{P}(t,\boldsymbol{\rho},z) = \int \mathrm{d}^2\rho' \int_{-\infty}^{0} \mathrm{d}z' \int \mathrm{d}t' \widehat{\chi}_H(\tau,\bar{\boldsymbol{\rho}},z,z')\, \boldsymbol{E}(t',\boldsymbol{\rho}',z'), \tag{6}$$

where we have used the shorthand notations $\bar{\boldsymbol{\rho}} = \boldsymbol{\rho} - \boldsymbol{\rho}'$, $\tau = t - t'$ and the susceptibility tensor $\widehat{\chi}_H$ for the metallic half-space is given by:

$$\widehat{\chi}_H(t,\boldsymbol{\rho},z,z') = \widehat{M}^{(+)}\Big[\widehat{\chi}(t,\boldsymbol{\rho},z-z') + \widehat{\chi}(t,\boldsymbol{\rho},-z-z')\Big] + \widehat{M}^{(-)}\Big[\widehat{\chi}(t,\boldsymbol{\rho},z-z') - \widehat{\chi}(t,\boldsymbol{\rho},-z-z')\Big], \tag{7}$$

where we have introduced the matrices:

$$\widehat{M}^{(+)} = \begin{pmatrix} 1 & & \\ & 1 & \\ & & 0 \end{pmatrix} \quad \text{and} \quad \widehat{M}^{(-)} = \begin{pmatrix} 0 & & \\ & 0 & \\ & & 1 \end{pmatrix} \tag{8}$$

which project on the components tangential and normal to the surface, respectively. Further, we have defined $\boldsymbol{\rho} = \widehat{M}^{(+)}\boldsymbol{r}$ and $\widehat{\chi}$ is the bulk susceptibility tensor. Finally, we assume that in the frequency range of interest the magnetization is negligible such that for the magnetic fields we can write:

$$\boldsymbol{H} = \boldsymbol{B}. \tag{9}$$

The main approximation of the specular reflection model is that the bulk susceptibility $\widehat{\chi}$ is used to describe the electronic response up to the surface, although the potential barrier at the border of the metal will lead to a region with a reduced electron density near the surface. For a metallic half-space the electronic depletion is restricted to a small region near the surface that is typically only a few nm thin. In this paper we will neglect this effect.

C. Continuation of the fields in the metallic half-space to the entire space

The purpose of this section is to show that the fields $\boldsymbol{P}$ and $\boldsymbol{E}$ describing the behavior of the metal in the half-space $z < 0$ can be continued to the entire space in such a way that (6) becomes a convolution integral over the entire space when rewritten in terms of the continued functions. To this end we note that while $\boldsymbol{P}(t,\boldsymbol{\rho},z)$ in (6) represents the polarization in the metal only for $z < 0$, the expression on the r.h.s. of this equation is formally meaningful also for values $z > 0$. Thus, a natural continuation of the metallic polarization is to define a function $\widetilde{\boldsymbol{P}}$ which is defined in the entire space by the r.h.s. of (6). This is equivalent to:

$$\widetilde{\boldsymbol{P}}(t,\boldsymbol{\rho},z) = \boldsymbol{P}(t,\boldsymbol{\rho},z) \quad \text{for } z<0 \quad \text{and} \quad \widehat{M}^{(\pm)}\widetilde{\boldsymbol{P}}(t,\boldsymbol{\rho},z) = \pm\,\widehat{M}^{(\pm)}\widetilde{\boldsymbol{P}}(t,\boldsymbol{\rho},-z) \quad \text{for } z>0. \tag{10}$$

We continue the electric field with the same symmetry such that:

$$\widetilde{\boldsymbol{E}}(t,\boldsymbol{\rho},z) = \boldsymbol{E}(t,\boldsymbol{\rho},z) \quad \text{for } z<0 \quad \text{and} \quad \widehat{M}^{(\pm)}\widetilde{\boldsymbol{E}}(t,\boldsymbol{\rho},z) = \pm\,\widehat{M}^{(\pm)}\widetilde{\boldsymbol{E}}(t,\boldsymbol{\rho},-z) \quad \text{for } z>0. \tag{11}$$

By definition $\widetilde{\boldsymbol{P}}$ is given by the r.h.s of (6) and can be decomposed into two parts:

$$\widetilde{\boldsymbol{P}}(t,\boldsymbol{\rho},z) = \widetilde{\boldsymbol{P}}_<(t,\boldsymbol{\rho},z) + \widetilde{\boldsymbol{P}}_>(t,\boldsymbol{\rho},z), \tag{12}$$

where $\widetilde{\boldsymbol{P}}_<$ collects the contributions to the half-space susceptibility (7) where the bulk susceptibility $\widehat{\chi}$ is evaluated with the argument $z - z'$. Using

$$\widehat{M}^{(+)} + \widehat{M}^{(-)} = \widehat{1} \tag{13}$$

and (11) we find:

$$\widetilde{\boldsymbol{P}}_<(t, \boldsymbol{\rho}, z) = \int \mathrm{d}^2\rho' \int_{-\infty}^{0} \mathrm{d}z' \int \mathrm{d}t' \widehat{\chi}(\tau, \bar{\boldsymbol{\rho}}, z - z')\, \widetilde{\boldsymbol{E}}(t', \boldsymbol{\rho}', z'). \tag{14}$$

$\widetilde{\boldsymbol{P}}_>$ accounts for the remaining contributions to (7) where $\widehat{\chi}$ is evaluated with the argument $-z - z'$. We insert these parts into (6) and substitute in the z' integral $z' \to -z'$ to obtain:

$$\widetilde{\boldsymbol{P}}_>(t, \boldsymbol{\rho}, z) = \int \mathrm{d}^2\rho' \int_0^{\infty} \mathrm{d}z' \int \mathrm{d}t' \Big\{ \Big[\widehat{M}^{(+)} - \widehat{M}^{(-)}\Big] \widehat{\chi}(\tau, \bar{\boldsymbol{\rho}}, -z + z') \underbrace{\Big[\widehat{M}^{(+)} + \widehat{M}^{(-)}\Big]}_{=\widehat{1}} \Big\} \boldsymbol{E}(t', \boldsymbol{\rho}', -z'). \tag{15}$$

From (4) we deduce that:

$$\widehat{M}^{\pm} \widehat{\chi}(\tau, \bar{\boldsymbol{\rho}}, z) \widehat{M}^{\pm} = \widehat{M}^{\pm} \widehat{\chi}(\tau, \bar{\boldsymbol{\rho}}, -z) \widehat{M}^{\pm} \quad \text{and} \quad \widehat{M}^{\pm} \widehat{\chi}(\tau, \bar{\boldsymbol{\rho}}, z) \widehat{M}^{\mp} = -\widehat{M}^{\pm} \widehat{\chi}(\tau, \bar{\boldsymbol{\rho}}, -z) \widehat{M}^{\mp}. \tag{16}$$

Using (16) together with (11) and (13) on the r.h.s of (15) we obtain:

$$\widetilde{\boldsymbol{P}}_>(t, \boldsymbol{\rho}, z) = \int \mathrm{d}^2\rho' \int_0^{\infty} \mathrm{d}z' \int \mathrm{d}t' \widehat{\chi}(\tau, \bar{\boldsymbol{\rho}}, z - z')\, \widetilde{\boldsymbol{E}}(t', \boldsymbol{\rho}', z'). \tag{17}$$

such that with (12) and (14) we finally find:

$$\widetilde{\boldsymbol{P}}(t, \boldsymbol{r}) = \int \mathrm{d}^3 r' \int \mathrm{d}t' \widehat{\chi}(t - t', \boldsymbol{r} - \boldsymbol{r}')\, \widetilde{\boldsymbol{E}}(t', \boldsymbol{r}') \tag{18}$$

demonstrating that the continued functions $\widetilde{\boldsymbol{P}}$ and $\widetilde{\boldsymbol{E}}$ are connected by the same relation as the functions $\boldsymbol{P}$ and $\boldsymbol{E}$ for a bulk metal in (5).

D. Maxwell equations for the continued fields

In order to proceed we introduce the electric displacement field $\widetilde{\boldsymbol{D}}$ that is connected with the continued fields $\widetilde{\boldsymbol{E}}$ and $\widetilde{\boldsymbol{P}}$ by:

$$\widetilde{\boldsymbol{D}} = \widetilde{\boldsymbol{E}} + 4\pi\, \widetilde{\boldsymbol{P}}, \tag{19}$$

implying that $\widetilde{\boldsymbol{D}}$ continues the electric displacement field $\boldsymbol{D}$ inside the metal to the entire space with the same symmetry as stated for $\widetilde{\boldsymbol{E}}$ and $\widetilde{\boldsymbol{P}}$ in (10) and (11). Since $\widetilde{\boldsymbol{D}}$ coincides with $\boldsymbol{D}$ for $z < 0$ it has to obey $\mathrm{div}\widetilde{\boldsymbol{D}} = 0$ for $z < 0$. The symmetry of the continuation guarantees that this equation also holds for $z > 0$. At this point it is important to recall that $\widetilde{\boldsymbol{D}}$ for $z > 0$ is not the physical field $\boldsymbol{D}$ which describes in this region the local response of a simple dielectric. In particular, the normal component of $\boldsymbol{D}$ is required by the usual continuity relations for the Maxwell equations to be continuous at the surface, i.e.:

$$\boldsymbol{D}_z(t, \boldsymbol{\rho}, z = 0^+) = \boldsymbol{D}_z(t, \boldsymbol{\rho}, z = 0^-) = \widetilde{\boldsymbol{D}}_z(t, \boldsymbol{\rho}, z = 0^-). \tag{20}$$

On the other hand, $\widetilde{\boldsymbol{D}}_z$ being defined for $z > 0$ as the anti-symmetric continuation of $\boldsymbol{D}_z$ for $z < 0$ may exhibit a discontinuity at the surface given by:

$$4\pi\sigma(t, \boldsymbol{\rho}) = \widetilde{\boldsymbol{D}}_z(t, \boldsymbol{\rho}, z = 0^+) - \widetilde{\boldsymbol{D}}_z(t, \boldsymbol{\rho}, z = 0^-) = -2\widetilde{\boldsymbol{D}}_z(t, \boldsymbol{\rho}, z = 0^-). \tag{21}$$

We note in passing that the the discontinuity in (21) is not the discontinuity of the real field on the both sides of the interface - it is the discontinuity between the field and its mirror reflection at the interface. Thus, this condition is

not the ABC for real fields.[1] It is a consequence of the continuation of the EM problem onto the entire space. The discontinuity results in a singular contribution to $\mathrm{div}\widetilde{\boldsymbol{D}}$ such that:

$$\mathrm{div}\widetilde{\boldsymbol{D}} = 4\pi\,\delta(z)\,\sigma(t,\boldsymbol{\rho}). \tag{22}$$

Next we introduce the continuation of the magnetic field in the metal as:

$$\widetilde{\boldsymbol{B}}(t,\boldsymbol{\rho},z) = \boldsymbol{B}(t,\boldsymbol{\rho},z) \quad \text{for } z<0 \quad \text{and} \quad \widehat{M}^{(\pm)}\widetilde{\boldsymbol{B}}(t,\boldsymbol{\rho},z) = \mp\,\widehat{M}^{(\pm)}\widetilde{\boldsymbol{B}}(t,\boldsymbol{\rho},-z) \quad \text{for } z>0, \tag{23}$$

which implies that:

$$\mathrm{rot}\widetilde{\boldsymbol{E}} = -\frac{1}{c}\,\dot{\widetilde{\boldsymbol{B}}}. \tag{24}$$

For $z<0$ (24) is just one of the Maxwell equations in the metal. The symmetries (11) and (23) guarantee that (24) also holds for $z>0$. Here, no singular contribution occurs since only $\widetilde{\boldsymbol{E}}_z$ exhibits a discontinuity and the l.h.s. of (24) does not contain a z-derivative of this component.

Since the tangential components of $\widetilde{\boldsymbol{B}}$ are defined as an odd continuation with respect to z, they may exhibit a jump at $z=0$ given by:

$$\frac{4\pi}{c}\boldsymbol{\beta}(t,\boldsymbol{\rho}) = \widehat{M}^{(+)}\big[\widetilde{\boldsymbol{B}}(t,\boldsymbol{\rho},z=0^+) - \widetilde{\boldsymbol{B}}(t,\boldsymbol{\rho},z=0^-)\big] = -2\widehat{M}^{(+)}\widetilde{\boldsymbol{B}}(t,\boldsymbol{\rho},z=0^-) =: \frac{4\pi}{c}\begin{pmatrix}\beta_x\\ \beta_y\\ 0\end{pmatrix}. \tag{25}$$

Obviously, this jump does not introduce singular contributions to $\mathrm{div}\widetilde{\boldsymbol{B}}$. From Maxwells equations and noting that the symmetry (23) implies that $\mathrm{div}\widetilde{\boldsymbol{B}}$ is an odd function of z we find that:

$$\mathrm{div}\widetilde{\boldsymbol{B}} = 0 \tag{26}$$

holds in the entire space. The discontinuity (25) leads to a singular surface contribution to $\mathrm{rot}\widetilde{\boldsymbol{B}}$ that can be written as:

$$\frac{4\pi}{c}\,\delta(z)\,\boldsymbol{j}(t,\boldsymbol{\rho}) = \frac{4\pi}{c}\,\delta(z)\begin{pmatrix}-\beta_y(t,\boldsymbol{\rho})\\ \beta_x(t,\boldsymbol{\rho})\\ 0\end{pmatrix}, \tag{27}$$

such that the Maxwell equation for $\mathrm{rot}\widetilde{H} = \mathrm{rot}\widetilde{B}$ turns into:

$$\mathrm{rot}\widetilde{\boldsymbol{B}} = \frac{4\pi}{c}\,\delta(z)\,\boldsymbol{j}(t,\boldsymbol{\rho}) + \frac{1}{c}\,\dot{\widetilde{\boldsymbol{D}}}. \tag{28}$$

Finally, writing the Maxwell equations for the continued fields in Fourier space we obtain:

$$i\boldsymbol{k}\cdot\widetilde{\boldsymbol{D}}_{\omega,\boldsymbol{k}} = 4\pi\,\sigma_{\omega,\boldsymbol{q}} \tag{29a}$$

$$i\boldsymbol{k}\times\widetilde{\boldsymbol{E}}_{\omega,\boldsymbol{k}} = i\frac{\omega}{c}\,\widetilde{\boldsymbol{B}}_{\omega,\boldsymbol{k}} \tag{29b}$$

$$i\boldsymbol{k}\cdot\widetilde{\boldsymbol{B}}_{\omega,\boldsymbol{k}} = 0 \tag{29c}$$

$$i\boldsymbol{k}\times\widetilde{\boldsymbol{B}}_{\omega,\boldsymbol{k}} = \frac{4\pi}{c}\,\boldsymbol{j}_{\omega,\boldsymbol{q}} - \frac{i\omega}{c}\,\widetilde{\boldsymbol{D}}_{\omega,\boldsymbol{k}}, \tag{29d}$$

where $\boldsymbol{q} = \widehat{M}^{(+)}\boldsymbol{k}$ is the part of $\boldsymbol{k}$ tangential to the surface. Furthermore, we have the material equation:

$$\widetilde{\boldsymbol{D}}_{\omega,\boldsymbol{k}} = \widehat{\varepsilon}_{\omega,\boldsymbol{k}}\widetilde{\boldsymbol{E}}_{\omega,\boldsymbol{k}}, \quad \text{with} \quad \widehat{\varepsilon}_{\omega,\boldsymbol{k}} = \widehat{1} + 4\pi\,\widehat{\chi}_{\omega,\boldsymbol{k}}, \tag{30}$$

which follows from (19) and (18) where $\widehat{\chi}$ has to be taken from (2).

The solution of (29) is most easily found by decomposing all fields into longitudinal and transverse parts. Using (2) the action of the dielectric tensor $\widehat{\varepsilon}$ simplifies to:

$$\widetilde{\boldsymbol{D}}_{\omega,\boldsymbol{k}} = \widehat{\varepsilon}_{\omega,\boldsymbol{k}}\cdot\widetilde{\boldsymbol{E}}_{\omega,\boldsymbol{k}} = \varepsilon^{\ell}_{\omega,k}\,\widetilde{\boldsymbol{E}}^{\ell}_{\omega,\boldsymbol{k}} + \varepsilon^{\mathrm{tr}}_{\omega,k}\,\widetilde{\boldsymbol{E}}^{\mathrm{tr}}_{\omega,\boldsymbol{k}}, \tag{31}$$

where $\widetilde{\boldsymbol{E}}^{\ell}$ and $\widetilde{\boldsymbol{E}}^{\rm tr}$ denote the longitudinal and transverse parts of $\widetilde{\boldsymbol{E}}$, respectively. With the help of (31) the Maxwell equations (29) naturally separate into simple algebraic equations for the longitudinal and transverse field components. Solving for the electric fields we obtain:

$$\widetilde{\boldsymbol{E}}^{\ell}_{\omega,\boldsymbol{k}} = \boldsymbol{k}\,\frac{4\pi\,\sigma_{\omega,\boldsymbol{q}}}{ik^2\varepsilon^{\ell}_{\omega,k}} \tag{32a}$$

$$\widetilde{\boldsymbol{E}}^{\rm tr}_{\omega,\boldsymbol{k}} = \frac{4\pi\,\frac{w}{c^2}}{i\big(\frac{w^2}{c^2}\varepsilon^{\rm tr}_{\omega,k}-k^2\big)}\,\Big(\boldsymbol{j}_{\omega,\boldsymbol{q}} - \boldsymbol{k}\frac{\omega\sigma_{\omega,\boldsymbol{q}}}{k^2}\Big) \tag{32b}$$

Once $\widetilde{\boldsymbol{E}}$ is known the magnetic field is found from (29b).

II. SOLUTION TO THE SCATTERING PROBLEM

A. Reflection coefficient for TM polarization

We consider a geometry as sketched in Fig. 1 in the main text, where an incident wave is approaching the surface of a metal at an angle θ coming from a dielectric in the half-space $z>0$ with a wave vector $\boldsymbol{k}^{\rm in}$ and a reflected wave with wave vector $\boldsymbol{k}^{\rm re}$ such that:

$$\boldsymbol{k}^{\rm in} = k^{\rm in}\begin{pmatrix}\sin(\theta)\\0\\-\cos(\theta)\end{pmatrix},\quad \boldsymbol{k}^{\rm re} = k^{\rm in}\begin{pmatrix}\sin(\theta)\\0\\\cos(\theta)\end{pmatrix}. \tag{33}$$

The TM (p) wave reflection corresponds to the case where the incoming and reflected electric fields have only components lying in the plane spanned by $\boldsymbol{k}_{\rm in}$ and $\boldsymbol{k}_{\rm re}$. Since in a simple dielectric the $\boldsymbol{k}$-vector has to be orthogonal to the field we can write the electric field of a p wave in the half-space $z>0$ as:

$$\boldsymbol{E}(t,\boldsymbol{r}) = E_0 e^{i(q^{\rm in}x-\omega^{\rm in}t)}\Big[R\,e^{ik_z^{\rm in}z}\begin{pmatrix}\cos(\theta)\\0\\-\sin(\theta)\end{pmatrix} - e^{-ik_z^{\rm in}z}\begin{pmatrix}\cos(\theta)\\0\\\sin(\theta)\end{pmatrix}\Big], \tag{34}$$

where R is the reflection coefficient, $q^{\rm in}=k^{\rm in}\sin(\theta)$, and $k_z^{\rm in}=k^{\rm in}\cos(\theta)$ with $(k^{\rm in})^2=(q^{\rm in})^2+(k_z^{\rm in})^2=\varepsilon_h(\omega^{\rm in}/c)^2$, where ε_h is the dielectric constant of the dielectric half-space. The electric displacement for $z>0$ is given by

$$\boldsymbol{D}(t,\boldsymbol{r}) = \varepsilon_h\,\boldsymbol{E}(t,\boldsymbol{r}). \tag{35}$$

and the magnetic field is obtained from the Maxwell equations as

$$\boldsymbol{B}(t,\boldsymbol{r}) = \frac{cE_0k^{\rm in}}{\omega^{\rm in}}\Big(e^{i\boldsymbol{k}^{\rm in}\boldsymbol{r}} + R\,e^{i\boldsymbol{k}^{\rm re}\boldsymbol{r}}\Big)\boldsymbol{e}_y e^{-i\omega^{\rm in}t}, \tag{36}$$

where $\boldsymbol{e}_y$ is the unit vector in y-direction. Now we have to match the solutions in both media at the interface. The continuity of D_z yields the surface charge as

$$\sigma_{\omega,\boldsymbol{q}} = (2\pi)^2\varepsilon_h E_0\sin(\theta)(R+1)\delta(\boldsymbol{q}-q^{\rm in}\boldsymbol{e}_x)\,\delta(\omega-\omega^{\rm in}), \tag{37}$$

with $\boldsymbol{e}_x$ being the unit vector in x-direction. The continuity of the tangential components of $\boldsymbol{B}$ yields the current

$$\boldsymbol{j}_{\omega,\boldsymbol{q}} = \frac{(2\pi c)^2E_0k^{\rm in}}{\omega^{\rm in}}\,\delta(\boldsymbol{q}-q^{\rm in}\boldsymbol{e}_x)\delta(\omega-\omega^{\rm in})(R+1)\boldsymbol{e}_x. \tag{38}$$

The continuity of B_z is trivially fulfilled for p waves since this component is zero on both sides of the surface. Finally, the tangential component of $\boldsymbol{E}$ is to be matched with the tangential component of the field in the dielectric. This yields

$$\boldsymbol{E}_t(t,\boldsymbol{\rho},0^-) = E_0\cos(\theta)e^{i(q^{\rm in}x-\omega^{\rm in}t)}(R-1)\boldsymbol{e}_x, \tag{39}$$

where the field on the metal side is given by the solution of the Maxwell equations with the surface charge density and current defined above. Resolving this equation for R one finds the reflection coefficient given in Eq. 1 of the main text, where in the final expression we have renamed $q^{\rm in}$, $\omega^{\rm in}$ and R in q, ω and R_p, respectively.

B. Reflection coefficient for TE polarization

In this case the wave vectors of the incoming and reflected waves are again given by (33). For a TE wave the electric field is linearly polarized perpendicular to the plane spanned by $\boldsymbol{k}^{\mathrm{in}}$ and $\boldsymbol{k}^{\mathrm{re}}$, i.e. in our case in y-direction. We thus can write

$$\boldsymbol{E}(t,\boldsymbol{r}) = E_0 \left(e^{i\boldsymbol{k}^{\mathrm{in}}\cdot\boldsymbol{r}} + R\, e^{i\boldsymbol{k}^{\mathrm{re}}\cdot\boldsymbol{r}} \right) \boldsymbol{e}_y\, e^{-i\omega^{\mathrm{in}}t}. \tag{40}$$

In this case $D_z = 0$ for $z > 0$ and therefore $\sigma_{\omega,\boldsymbol{q}} = 0$. The corresponding magnetic field is found as

$$\boldsymbol{B}(t,\boldsymbol{r}) = \frac{cE_0 k^{\mathrm{in}}}{\omega^{\mathrm{in}}}\, e^{i(q^{\mathrm{in}}x - \omega^{\mathrm{in}}t)} \left[\begin{pmatrix} \cos(\theta) \\ 0 \\ \sin(\theta) \end{pmatrix} e^{-ik_z^{\mathrm{in}}z} + R \begin{pmatrix} -\cos(\theta) \\ 0 \\ \sin(\theta) \end{pmatrix} e^{ik_z^{\mathrm{in}}z} \right]. \tag{41}$$

The continuity of the tangential component of the magnetic field yields

$$\begin{aligned} \boldsymbol{j}_{\omega,\boldsymbol{q}} =& \frac{(2\pi c)^2 E_0 k^{\mathrm{in}}}{\omega^{\mathrm{in}}} \cos(\theta)\,(R-1) \\ & \times \delta(\boldsymbol{q} - q^{\mathrm{in}}\boldsymbol{e}_x)\, \delta(\omega - \omega^{\mathrm{in}})\, \boldsymbol{e}_y. \end{aligned} \tag{42}$$

The continuity of the tangential component of the electric field yields

$$\boldsymbol{E}_t(t,\boldsymbol{\rho},0^-) = E_0\, e^{i(q^{\mathrm{in}}x - \omega^{\mathrm{in}}t)}(R+1)\boldsymbol{e}_y. \tag{43}$$

Now, using the solution to the Maxwell equations for the field together with the obtained expression for the surface current one obtains the reflection coefficient in Eq. 1 in the main text. We note in passing that in this case the continuity of B_z leads to the same condition as the continuity of the tangential component of the electric field.

III. INTER-BAND TRANSITIONS

Transitions of carriers between different conduction bands in metals provide additional contributions to the metal permittivity. These are typically active in the visible and near-violet spectral range for noble metals and can distort the contribution of the electron gas (intra-band transitions) in the SASE domain. The common approach consists in separating the intra-band effects from inter-band effects[2]. The contribution of the inter-band transitions is assumed to be local. Following Cardona[3] they can be modeled by the following dielectric susceptibility

$$\chi_\omega^{ib} = 4\pi \sum_{k=\mathrm{occupied}}^{l=\mathrm{empty}} \frac{F_{lk}}{\omega_{lk}^2 - (\omega + i\Gamma_{ib})^2} \tag{44}$$

respectively, ω_{lk} is the transition frequency, $F_{lk} \sim |p_{kl}|^2 / \omega_{lk}$ is the oscillator strength with p_{kl} being the matrix element of the momentum operator, and Γ_{ib} is a broadening factor due to particle scattering. In this model, every transition between an occupied state and an empty state contributes an extra Lorentzian oscillator to the dielectric function. It should be noted that a satisfactory description using this expression often requires an exceedingly large number of Lorentzian terms with fitted parameters[4–9].

To select the most contributing transitions from the physical perspective Etchegoin et al. have proposed to use the Critical Points model[10], which has been successfully employed for the analysis of inter-band transitions in semiconductors[11] as well as in noble and transition metals[12–15]. It was later improved by taking into account the band structure of the metals[16,17]. In this model one assumes that the matrix element in the oscillator strength varies slowly around the transition points and that the only dependence on the states is given by ω_{lk}^{-1}[3]. It is further assumed that Γ_{ib} is constant for each transition point and that only direct transitions are accounted for. Under these assumptions the summation in Eq. (44) can be replaced by an integration over the joint density of states (jDOS) $J_j(\omega)$ (j denotes the critical point). The jDOS may be expressed as an integral over the density of states for the bands involved in the transition

$$J_j(\omega) = \int_{-\infty}^{\infty} N_{j,1}(E)\, N_{j,2}(E + \hbar\omega)\, dE \tag{45}$$

where $N_{j,1}(E)$ and $N_{j,2}(E)$ denote the DOS for the initial (j,1) and the final (j,2) bands at the critical point j. The total contribution to the susceptibility is then found as

$$\chi_{\omega}^{ib} = \sum_{j} A_j \int_0^{\infty} \frac{J_j(\xi)}{\xi^2 - (\omega + i\Gamma_j)^2} \frac{d\xi}{\xi}, \tag{46}$$

where the sum runs over the contributing critical points.

It follows from DFT band calculations,[16] that the relevant critical points of metallic silver are located in the visible energy range at the X and L symmetry points. The dispersion of the transition energy around those points is assumed quadratic with three effective masses. The critical point at X has a gap of about 4.0 eV for Ag and it is of M_1 type[3] with one negative and two positive effective masses along the primary axes. The corresponding jDOS is given by

$$J_1(\omega) \propto \begin{cases} 0, & \omega < \omega_{01} \\ \sqrt{\omega_{g1} - \omega_{01}} - \sqrt{\omega_{g1} - \omega}, & \omega_{01} < \omega < \omega_{g1} \\ \sqrt{\omega_{g1} - \omega_{01}}, & \omega > \omega_{g1} \end{cases}, \tag{47}$$

where ω_{g1} are ω_{01} parameters of the band. Substituting this into the expression for the susceptibility one obtains the following expression

$$\chi_1^{ib}(\omega) = A_1 \left\{ -\frac{\sqrt{\omega_{g1} - \omega_{01}}}{2(\omega + i\Gamma_1)^2} \ln\left[1 - \left(\frac{\omega + i\Gamma_1}{\omega_{01}}\right)^2\right] + \frac{2\sqrt{\omega_{g1}}}{(\omega + i\Gamma_1)^2} \tanh^{-1}\sqrt{\frac{\omega_{g1} - \omega_{01}}{\omega_{g1}}} \right.$$
$$\left. - \frac{2\sqrt{\omega + i\Gamma_1 - \omega_{g1}}}{(\omega + i\Gamma_1)^2} \tan^{-1}\sqrt{\frac{\omega_{g1} - \omega_{01}}{\omega + i\Gamma_1 - \omega_{g1}}} - \frac{2\sqrt{\omega + i\Gamma_1 + \omega_{g1}}}{(\omega + i\Gamma_1)^2} \tanh^{-1}\sqrt{\frac{\omega_{g1} - \omega_{01}}{\omega + i\Gamma_1 + \omega_{g1}}} \right\} \tag{48}$$

At the L symmetry point, the gap is slightly above 4.0eV. This critical point is of M_2 type[3] having two negative and one positive effective masses. The jDOS in this case can be approximated as

$$J_2(\omega) \propto \begin{cases} 0, & \omega < \omega_{02} \\ 1, & \omega > \omega_{02} \end{cases}. \tag{49}$$

The corresponding contribution to the susceptibility is obtained as

$$\chi_2^{ib}(\omega) = \frac{A_2}{2(\omega + i\Gamma_2)^2} \ln\left[1 - \left(\frac{\omega + i\Gamma_2}{\omega_{02}}\right)^2\right] \tag{50}$$

Parameters of each contributing point (ω_{0j}, ω_{gj}, Γ_j, and A_j) are usually found by fitting experimental data. In our calculations we have taken those parameters from Ref.[16,17] summarized in table I.

	ω_{gj}(eV)	ω_{0j}(eV)	Γ_j(eV)	A_{M_j}(eV$^{3/2}$)
j=1	4.06	3.93	0.018	191
j=2	–	4.17	0.19	31

TABLE I. Parameters for the dielectric response of the inter-band transitions in Ag. ω_{g2} is not required for Eq. (50).

IV. ANALYTICAL ESTIMATIONS FOR THE SASE PEAK

We derive an analytical estimation for the SASE contribution to the absorptivity as given by Eqs. (15) and (16) in the main text. In what follows we use the scaled units so that the frequency becomes $\bar{\omega} \to \alpha\omega$, and the absolute value of the EM wave vector writes as $k = \alpha\omega$ and its tangential component is $q = \cos(\theta)\alpha\omega$.

Calculating the respective integral for the Drude contribution Z_p^D in Eq. (16) in the mains text to the surface impedance one obtains

$$Z_p^D = \frac{i}{\cos(\theta)} \frac{\sqrt{-\varepsilon_{\omega}^D + \sin^2(\theta)}}{\varepsilon_{\omega}^D}. \tag{51}$$

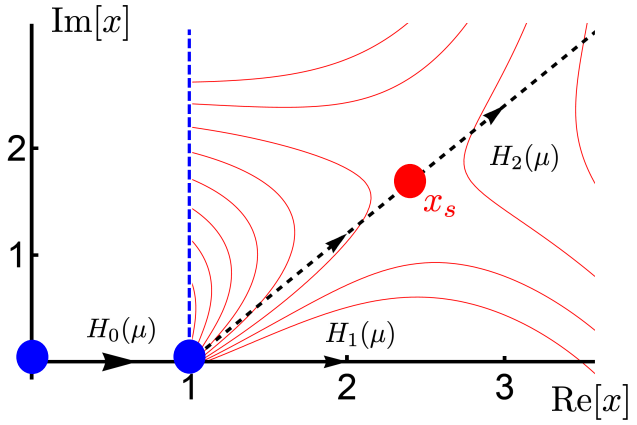

FIG. 1. Contours for the evaluation of $H_0(\mu), H_1(\mu)$ (solid lines) and $H_2(\mu)$ (dashed line). Red contours correspond to $|f(x,\mu)|^{-1}$ with the saddle point x_s. Blue dashed line is the cut for the $\ln(x-1)$ function.

The real part of this expression gives in the limit of small $\gamma \ll \omega$

$$\mathrm{Re}[Z_p^D] \simeq \frac{\gamma}{2\cos(\theta)} \frac{1+\omega^2-2\omega^2\cos^2(\theta)}{(1-\omega^2)^2\sqrt{1-\omega^2\cos^2(\theta)}}. \tag{52}$$

Equation (15) in the main text for the corrective term can be further simplified by noting that here one needs only the imaginary part. Using the fact that the integrand in Eq. (15) in the main text is an even function of k_z and substituting $k = (\omega + i\gamma)x$ we represent the integral in Eq. (15) in the main text as

$$\int_0^\infty \frac{dk}{k^2}\left(\frac{1}{\varepsilon^\ell_{\omega k}} - \frac{1}{\varepsilon^D_\omega}\right) = \frac{1}{(\omega+i\gamma)} H(\mu) \tag{53}$$

where

$$H(\mu) = \int_0^\infty \left[\frac{1}{f(x,\mu)} + \frac{1}{x^2(\mu^2-1)}\right] dx, \tag{54}$$

$\mu^2 = [\omega(\omega+i\gamma)]^{-1}$ and

$$f(x,\mu) = x^2 + 3\mu^2\left[1 - \frac{1}{2x}\log\left(\frac{x+1}{1-x}\right)\right]. \tag{55}$$

The behavior of the function $1/f(x,\mu)$ is shown in Fig. 1 in the complex x-plane. This function has logarithmic branching points at $x = \pm 1$, the branch cut line is chosen to go vertically, upwards from $x = 1$. This integral can be estimated by the saddle-point method by shifting the integration contour to the complex space. To do this we first split the integration interval to $[0,1]$ and $[1,\infty)$. The first integral

$$H_0(\mu) = \int_0^1 \left[\frac{1}{f(x,\mu)} + \frac{1}{x^2(\mu^2-1)}\right] dx \tag{56}$$

has a very small imaginary part at large μ where it has the asymptotic $H_0(\mu) \propto 1/\mu^2$.

The integral in the second interval writes as

$$H_1(\mu) = H_2(\mu) + \frac{1}{\mu^2-1}, \tag{57}$$

where the second contribution is the result of the exact integration of the second term in the integrand in Eq. (54) and

$$H_2(\mu) = \int_1^\infty \frac{dx}{x^2 + 3\mu^2\left[1 - \frac{1}{2x}\left(\ln\left(\frac{x+1}{x-1}\right) + i\pi\right)\right]}. \tag{58}$$

Here we used the explicit form of the imaginary part of $f(x,\mu)$ provided by the logarithm with a negative argument.

The value of this integral is evaluated by employing the stationary- or saddle-point approximation. To do this we first find the stationary point x_s of the function $f(x,\mu)$ by solving the equation $df(x,\mu)/dx = 0$. At large x this equation reads as

$$\frac{6\mu^2}{x^3} - \frac{3i\pi\mu^2}{2x^2} + 2x = 0. \tag{59}$$

The solution to this equation is obtained using the perturbation expansion assuming μ is large. It gives

$$x_s \simeq \frac{(3\pi i)^{1/3}\mu^{2/3}}{2^{2/3}} + \frac{4i}{3\pi}, \tag{60}$$

where we chose the most relevant solution. We then substitute the expansion of the function $f(x,\mu)$ in the vicinity of the stationary point into the integrand and deform the integration contour $\mathcal{C}$ into the complex plane as shown in Fig. 1 by the dashed line. Finally we extend the lower end of the integration contour also to infinity. This yields

$$H_2(\mu) \;\simeq\; \int_{\mathcal{C}} \frac{dx}{f(x_s) + f''(x_s)(x-x_s)^2/2} = \frac{\pi\sqrt{2}}{\sqrt{f(x_s)f''(x_s)}}, \tag{61}$$

where

$$f(x_s)f''(x_s) \simeq \frac{(3i)^{2/3}\left(16+9\pi^2\right)\mu^{4/3}}{2^{1/3}\pi^{4/3}} + 18\mu^2. \tag{62}$$

Further, for the chosen parameters $\mathrm{Im}[H_2(\mu)]$ dominates over both $\mathrm{Im}[1/(\mu^2-1)]$ and $\mathrm{Im}[H_0(\mu)]$ already at $\mu \gtrsim 1.2$. It is also possible to neglect the imaginary part of μ that is defined by the decay rate Γ. Substituting the results of Eqs. (62) and (61) into Eq. (15) in the main text and using $\mu \approx 1/\omega$ yields the estimate for the SASE contribution to the surface impedance as

$$\mathrm{Re}\left[\delta Z_p^S\right] \simeq \frac{2\alpha\,\omega^2\sin^2(\theta)}{3\cos(\theta)}\mathrm{Im}\left[\frac{1}{\sqrt{1+(1.04+1.8i)\omega^{2/3}}}\right], \tag{63}$$

where we substituted numerical values for the constants. Substituting the result into the absorptivity ratio in Eq. (16) in the main text together with the Drude approximation (51) one obtains

$$r_p^S \simeq 1 - \frac{4\alpha\,\omega\sin^2(\theta)}{3\gamma}\frac{(1-\omega^2)^2\sqrt{1-\omega^2\cos^2(\theta)}}{1+\omega^2-2\omega^2\cos^2(\theta)}\mathrm{Im}\left[\frac{1}{\sqrt{1+(1.04+1.8i)\omega^{2/3}}}\right] \tag{64}$$

This equation is already quite simple but can be reduced even further by neglecting $\omega \ll 1$ and $\cos(\theta)$. When one further uses the expansion with respect to ω and keeps the largest contribution one obtains Eq. (17) in the main text.

[1] S.I. Pekar, *The Theory of Electromagnetic Waves in a Crystal in which Excitons are Produced*, Sov. Phys. JETP **6** (33), 785 (1958).

[2] V. P. Drachev, U. K. Chettiar, A. V. Kildishev, H.-K. Yuan, W. Cai, and V. M. Shalaev, *The Ag dielectric function in plasmonic metamaterials*, Optics Express **16**, 1186 (2008).

[3] M. Cardona, *Solid State Physics: Modulation Spectroscopy*, (Academic Press, New York , NY, USA 1969).

[4] A. D. Rakic, A. B. Djurisic, J. M. Elazar, M. L. Majewski, *Optical properties of metallic films for vertical-cavity optoelectronic devices*, Appl. Opt. **37**, 5271 (1998).

[5] M. Moskovits, I. Srnová-Šloufova, B. Vlčková, *Bimetallic Ag–Au nanoparticles: Extracting meaningful optical constants from the surface-plasmon extinction spectrum*, J. Chem. Phys. **116**, 10435 (2002).

[6] K. C. See, J. B. Spicer, J. Brupbacher, D. Zhang, T. G. Vargo, *Modeling interband transitions in silver nanoparticle-fluoropolymer composites*, J. Phys. Chem. B **109**, 2693 (2005).

[7] T.-W. Lee, S. Gray, *Subwavelength light bending by metal slit structures*, Opt. Express **13**, 9652 (2005).

[8] F. Hao, P. Nordlander, *Efficient dielectric function for FDTD simulation of the optical properties of silver and gold nanoparticles*, Chem. Phys. Lett. 446, 115 (2007).

[9] O. Pena-Rodríguez. *Modelling the dielectric function of Au-Ag alloys*, Journal of Alloys and Compounds 694, 857 (2017).

[10] P. G. Etchegoin, E. C. Le Ru, M. Meyer, *An analytic model for the optical properties of gold*, J. Chem. Phys. **125**, 164705 (2006); Erratum: J. Chem. Phys. **125**, 164705 (2006)], J. Chem. Phys. **127**, 189901 (2007).
[11] P. Etchegoin, J. Kircher, M. Cardona, *Elasto-optical constants of Si*, Phys. Rev. B **47**, 10292 (1993).
[12] A. Vial, T. Laroche, *Description of dispersion properties of metals by means of the critical points model and application to the study of resonant structures using the FDTD method*, J. Phys. D. Appl. Phys. **40**, 7152 (2007).
[13] A. Vial, *Implementation of the critical points model in the recursive convolution method for modelling dispersive media with the finite-difference time domain method*, J. Opt. A Pure Appl. Opt. **9**, 745 (2007).
[14] A. Vial, T. Laroche, *Comparison of gold and silver dispersion laws suitable for FDTD simulations*, Appl. Phys. B **93**, 139 (2008).
[15] J.Y. Lu, Y.H. Chang, *Implementation of an efficient dielectric function into the finite difference time domain method for simulating the coupling between localized surface plasmons of nanostructures*, Superlattices Microstruct. **47**, 60 (2010).
[16] D. Rioux, S. Vallières, S. Besner, Ph. Muñoz, E. Mazur, and M. Meunier, *An Analytic Model for the Dielectric Function of Au, Ag, and their Alloys*, Adv. Optical Mater. (2013).
[17] O. Pena-Rodríguez, M. Caro, A. Rivera, J. Olivares, J.M. Perlado, A. Caro, *Optical properties of Au-Ag alloys: an ellipsometric study*, Opt. Mater. Express **4**, 403 (2014).
[18] F. Quéré, H. Vincenti, *Reflecting petawatt lasers off relativistic plasma mirrors: a realistic path to the Schwinger limit*, High Power Laser Sci. Eng. **9**, e6 (2021).
[19] A.A. Vlasov. *The vibrational properties of an electron gas.* Zh. Eksp. Teor. Fiz., **8**, 29 (1938).
[20] M. Abramowitz and I. A. Stegun, *Handbook of Mathematical Functions with Formulas, Graphs, and Mathematical Tables.* US Government Printing Office, Washington, 10th printing, with corrections (December 1972)
[21] V. N. Faddeeva and N. N. Terent'ev, *Tables of values of the function w(z) for complex argument.* Gosud. Izdat. Teh.-Teor. Lit., Moscow, 1954; English transl., Pergamon Press, New York, 1961.
[22] H. B. Nersisyan, M. E. Veysman, N. E. Andreev, and H. H. Matevosyan, *Dielectric function of a collisional plasma for arbitrary ionic charge*, Phys. Rev. E **89**, 033102 (2014)
[23] J.D. Huba, *NRL Plasma Formulary* (Naval Research Laboratory, Washington, DC, 2007), http://www.nrl.navy.mil/ppd/content/nrl-plasma-formulary
[24] W. Kruer, *The Physics of Laser Plasma Interactions*, (Addison-Wesley, Boston, 1988).